# Observation of Magic Numbers within $NO/NH_3$ Mixed Cluster Ions

**Dong Nam Shin, Robert L. DeLeon, and James F. Garvey***

*Department of Chemistry, Natural Science & Mathematics Building, State University of New York at Buffalo, Buffalo, New York 14260-3000*

*Received: May 27, 1998; In Final Form: August 3, 1998*

The metastable decomposition of photoionized $NO/NH_3$ clusters has been investigated employing a reflectron time-of-flight mass spectrometer. The metastable dissociation spectra of the most prominent cluster ion species $NO^+(NH_3)_n$ ($3 \leq n \leq 28$) show that the rate coefficient for the loss of one $NH_3$ molecule from the cluster rapidly increases up to $n = 13$ and thereafter is nearly independent of the cluster size. This is interpreted as evidence of a stable structure that consists of a central $NO^+$ ion surrounded by a first solvation shell of 12 $NH_3$ molecules.

## Introduction

There has been intense interest in methods to reduce the emission of NO into the atmosphere because of its role as a pollutant.[1−3] For any system designed to remove NO from exhaust stacks, it is known that the addition of $NH_3$ to a moist mixture of NO leads to enhanced removal of the NO.[4−6] However, a persistent difficulty that has plagued such processes is the complexity of the physical phenomena and chemical reactions that occur. For example, it is reported that, in addition to the anticipated gas-phase reactions, multiphase reactions are also likely to occur in this process.

Recently, a possible alternative ionic process involving the formation of a protonated nitrosamide ($H_3NNO^+$) has been suggested.[7,8] In this process, the fast proton-transfer reaction of the $H_3NNO^+$ ion produces nitrosamide ($H_2NNO$) as an intermediate species. Subsequent dissociation of $H_2NNO$ occurs through two main reaction pathways[1−3]

$$[H_2NNO] \rightarrow N_2 + H + OH \qquad \Delta H = -5.7 \text{ kcal mol}^{-1} \quad (1)$$

$$\rightarrow N_2 + H_2O \qquad \Delta H = -124.9 \text{ kcal mol}^{-1} \quad (2)$$

Therefore, the study of the chemical reactions of the mixed cluster ions of NO and $NH_3$ molecules should be helpful in understanding the chemical mechanisms occurring in this process. While several groups have reported a number of extensive investigations of homogeneous NO[9−12] and $NH_3$[12−16] clusters, to our knowledge, a study of the heterocluster system between NO and $NH_3$ molecules has not been performed.

In this paper, we report new observations on the $NO/NH_3$ mixed cluster ions generated by multiphoton ionization (MPI). We have measured the metastable decay rate coefficient as a function of cluster ion size, and these rate constants are found to be a strong function of the cluster size.

## Experimental Section

A detailed description of the reflectron time-of-flight mass spectrometer (RTOFMS) used in this work has been previously published.[17,18] The neutral heteroclusters are expanded through a pulsed nozzle (General Valve Co., IOTA ONE) which has an 800 $\mu$m orifice diameter. After skimming by a 1.0 mm conical skimmer located 1.5 cm away from the nozzle, the cluster beam is introduced into the ionization region of the RTOFMS and irradiated by an unfocused 248 nm laser beam (Lambda Physik, EMG101) with a pulse width of approximately 20 ns. Cluster ions generated by the laser are accelerated in a double electrostatic field to 4.2 keV and travel through a 140 cm long flight tube toward a double-stage reflectron (R.M. Jordan Co.) located at the top of the flight tube. After being reflected by the reflectron, the ions pass an additional 61 cm back to a dual microchannel plate (MCP) detector. To minimize collision-induced dissociation of the ions on their way to the detector, the pressure in the instrument is maintained below $5 \times 10^{-7}$ Torr during operation by means of a 370 L/s turbomolecular pump and a liquid nitrogen cryogenic pump. The detected ion signals are recorded by a transient digitizer (LeCroy 9310) coupled to an IBM-PC and are averaged typically over 5000 laser pulses to increase the signal-to-noise ratio.

The experiments were performed with a gas mixture consisting of 0.24−1.28% ammonia and 5.0% nitric oxide in 2.4 atm of Ar buffer gas. The 99.99% (anhydrous grade) ammonia gas was obtained from Linde Specialty Gases, and 5.0% nitric oxide gas (seeded in Ar) was obtained from Matheson Gases. All of these reagents were used without further purification.

## Results

Figure 1 shows the mass spectrum of a pulsed molecular beam expanded from a gas mixture containing 2.4 atm of Ar gas, 5.0% NO, and 1.28% $NH_3$. The most prominent homocluster ions in the low mass region are protonated ammonia clusters of the form $(NH_3)_nH^+$. Formation of these protonated cluster ions is the result of an intracluster ion−molecule reaction immediately following the ionization of the neutral ammonia clusters.[13−15] The observation of the anomalously large intensity of $(NH_3)_5H^+$ (A5 in Figure 1) is expected since this magic number has been found previously in several studies. No $(NO)_n^+$ ions are observed in the mass spectrum for $n > 3$, indicating that the presence of the ammonia effectively hampers the formation of the homogeneous NO cluster ions by ligand-exchange (switching) reactions: e.g., $(NO)_2^+ + NH_3 \rightarrow NO + NO^+(NH_3)$. Note that the binding energy of the $NO^+NH_3$ complex (30.7 kcal/mol)[19] is much larger than that of the $(NO)_2^+$ complex (16.1 kcal/mol);[20] therefore, the observed ion intensity distribution reflects these relative ion stabilities.[21,22]

S1089-5639(98)02373-1 CCC: $15.00 
Published on Web 09/10/1998

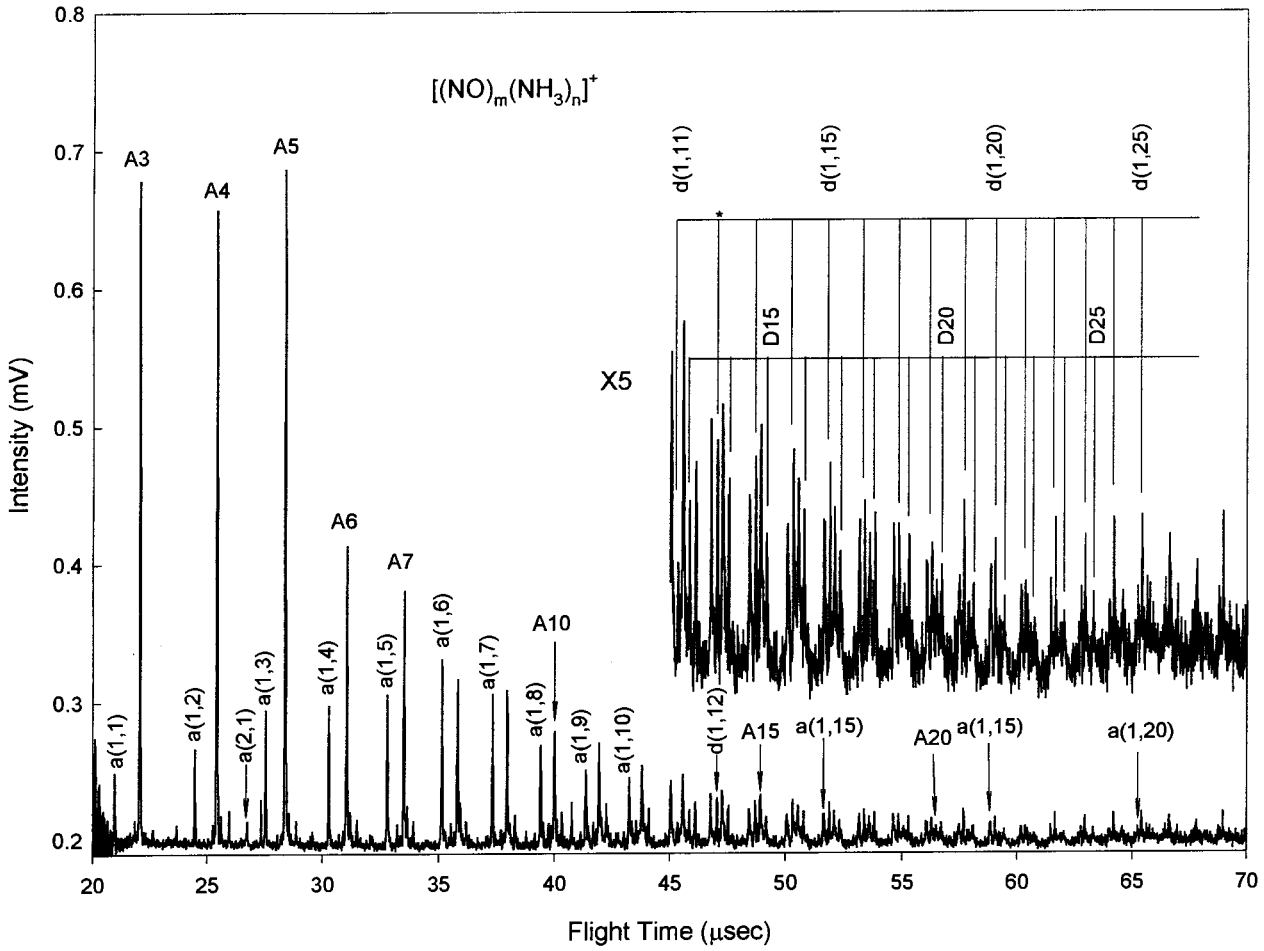


**Figure 1.** Typical mass spectrum of the NO (5%) and $NH_3$ (1.28%) mixed cluster seeded in 2.4 atm of Ar carrier gas. The protonated parent ammonia cluster and daughter ions of the form $(NH_3)_nH^+$ are designated by $A_n$ and $D_n$, respectively. The mixed cluster ion series and their daughter ions of the form $[(NO)_m(NH_3)_n]^+$ are designated by a($m$,$n$) and d($m$,$n$), respectively. Note the enhanced intensity of the parent ion at a(1,6) and of the daughter ion at d(1,12). Below 20 $\mu$s, there are large peaks due to monomers such as $Ar^+$ (40), $Ar^{2+}$ (20), $NO^+$ (30), $NH_3^+$ (14, 15, 16, and 17), and also $NH_4^+$ (18) and $(NH_3)_2H^+$ (35).

In addition to the homogeneous cluster ions, there are heterogeneous cluster ions of the form $[(NO)_m(NH_3)_n]^+$, as shown in Figure 1. Aside from the $[NO(NH_3)_n]^+$ series, only trace amounts of the $[(NO)_2(NH_3)]^+$ ion is observed. Although mixed cluster ions are observed up to $n = 50$, we have only displayed $n < 30$ in Figure 1. The intensity of the ions in the $[NO(NH_3)_n]^+$ series grows gradually as the number of ammonia molecules in the cluster increases from one to six and thereafter decreases monotonically.

Figure 2 shows the intensity distribution of the $[NO(NH_3)_n]^+$ ions as a function of the ammonia concentration at a fixed 5.0% concentration of NO. At $NH_3$ concentrations greater than 0.48%, the enhanced ion intensity centered at $n = 6$ is clearly observed. At the low concentrations, however, the enhanced ion intensity at $n = 6$ disappears, probably due to an insufficient number density of ammonia to form larger clusters which evaporate to form $[NO(NH_3)_6]^+$.

After ionization, the newly formed cluster ions in the ionization region undergo rapid fragmentation, reorganization, and evaporation. Since there is excess energy remaining in those cluster ions, further dissociation continues in the field-free region (FFR).[23] This metastable decay process should be studied in depth since it is capable of revealing detailed information on the individual cluster ion's stability.[24]

In the $NO/NH_3$ cluster system, two types of daughter cluster ions have been observed: one is generated from the loss of an ammonia molecule from the homogeneous cluster ions $(NH_3)_nH^+$ (denoted by "D"); the second is from the loss of an ammonia molecule from the heterogeneous cluster ions $[NO(NH_3)_n]^+$ (denoted by "d"). As shown in Figure 1, the peaks corresponding to daughter ions, d and D, are shifted to smaller ion arrival times than their parent ions because of their lower kinetic energy. Intensities of protonated ammonia and mixed cluster ions gradually diminish with increasing cluster size, yet their daughter cluster ions become relatively more intense. Note that the intensity of d(1,12) is anomalously large in the mixed daughter cluster ions.

The mixed daughter ions are generated via metastable dissociation in the FFR of the mass spectrometer. Stace and Moore have previously described the technique of using daughter ion metastable decay spectra to detect magic numbers.[25] Figure 3 displays the ratio of daughter intensity to parent plus daughter intensity as a function of cluster size for several ammonia concentrations. Examination of the relative intensity distribution for the metastable decay shows that the intensity of the loss of one ammonia in going from $n = 12$ to $n = 13$ increases quite abruptly. There is also a small decrease at $n = 8$. These abrupt changes in the ion intensity we feel are due to stable ion structures at $n = 12$ and $n = 8$. However, note that we did not observe a sudden drop in the relative intensity at $n = 6$ to correlate with the observed magic number in the parent mass spectrum.

The rate equation for the generation of the daughter ion, $i$, from its parent ion, $i + 1$, is given by

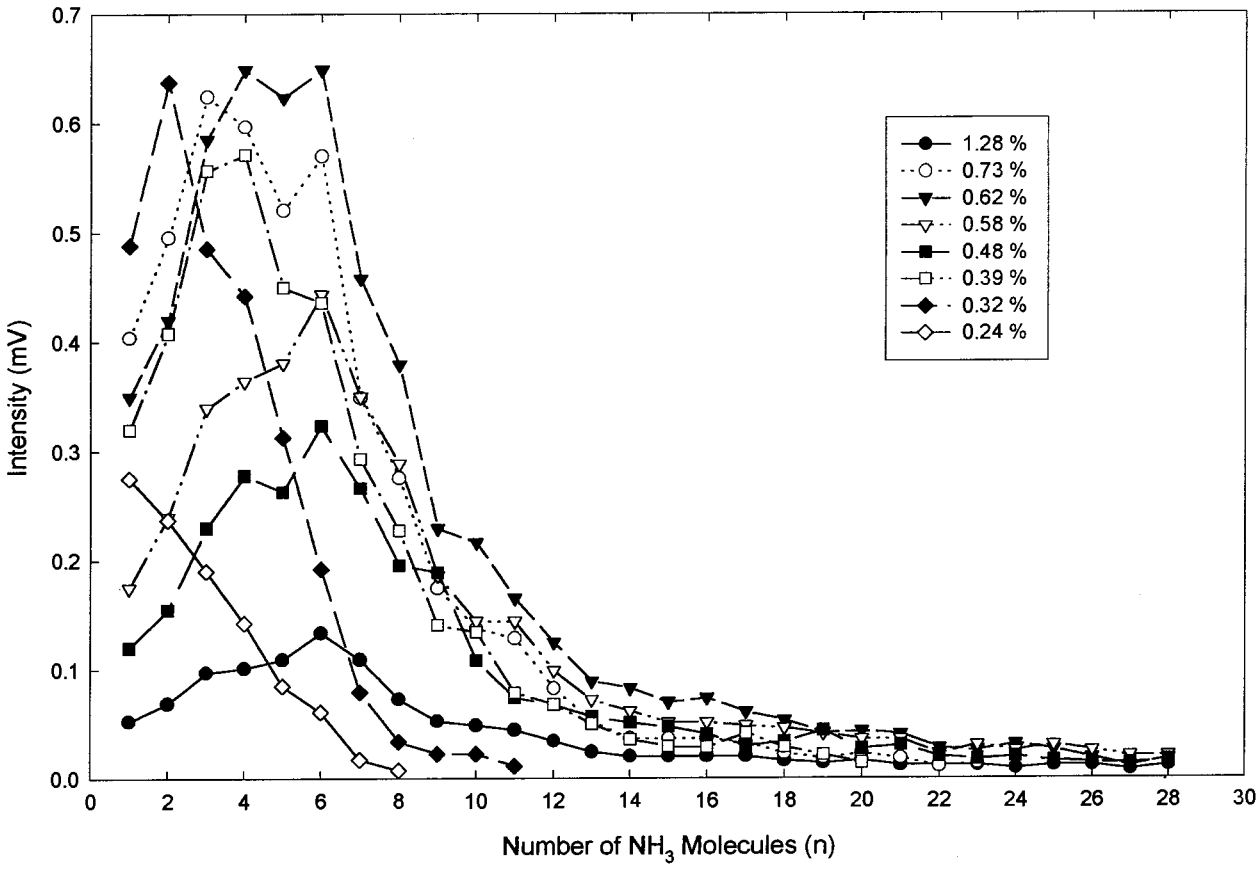


**Figure 2.** Intensity distribution of the mixed cluster ions $NO^+(NH_3)_n$ as a function of the ammonia cluster size at several different concentrations of ammonia.

$$d[D]/dt = k_p[P] - k_d[D] \quad (3)$$

where [P] and [D] are the intensity of parent and its daughter ions, and $k_p$ and $k_d$ are the rate coefficients of parent and daughter ions for the decay processes, respectively. As shown in Figure 1, we do not observe evaporation of $NH_3$ monomers to generate the $[NO(NH_3)_{n-2}]^+$ daughter ion from the $[NO(NH_3)_n]^+$ parent ion, possibly because there is insufficient excess energy for such successive evaporations. Therefore, the rate coefficient $k_d$ for any further loss can be dropped. With this simplification, the metastable rate equation can be integrated to determine the rate coefficients:

$$k_p = \ln\{1 + ([D]/[P])\}/\Delta t \quad (4)$$

where $\Delta t$ is the flight time that the parent ion spends in the FFR before entering the reflectron. Figure 4 displays the rate constants of the dissociation of the parent ion as a function of cluster size calculated using eq 4. The rate coefficients increase rapidly with increasing cluster size up to $n = 13$. Thereafter, the rate coefficients are nearly independent of the cluster size. Note that the rate coefficient $k_{13}$ increases abruptly over $k_{12}$ and that of $k_8$ decreases abruptly, indicating the special stability in the cluster ions $[NO(NH_3)_8]^+$ and $[NO(NH_3)_{12}]^+$.

## Discussion

The key step for the ionic DeNO*x* process in flames has been recently suggested to involve the generation of the $NH_3NO^+$ ion.[7,8] However, $NH_3NO^+$ has not been observed in flames. The absence of the $NH_3NO^+$ ion has been suggested to be due to fast proton-transfer reactions between $NH_3NO^+$ and $NH_3$ or $H_2O$ species to form $H_2NNO$ and $NH_4^+$ or $H_3O^+$, respectively.

Table 1 presents the relative energy differences in the reaction channels for the dissociation of the $NO^+(NH_3)_2$ ion as representative of the energetics of the $NO/NH_3$ system explored in this study. Four possible reaction channels of the $NO^+(NH_3)_2$ ion decomposition are considered. The generation of $NH_4^+$ and $NH_2NO$ species is the lowest energy channel, which is 10.4 kcal/mol lower than that of channel 2 generating $NH_3NO^+$ and $NH_3$. If a reaction such as channel 1 is dominant within the cluster molecular beam system, as is observed in flame studies, there is the possibility of the generation of protonated mixed cluster ions, in which the ion core is $NH_4^+$ solvated by $NH_3$ and NO molecules. In our present study, however, we note that we have observed only unprotonated mixed cluster ions, $[NO(NH_3)_n]^+$. This observation leads us to conclude that there will be an activation energy barrier to generate the $NH_4^+$ ion which is much larger than the barrier of channel 2. In the case of the flame environment, the energy barrier will be unimportant because the temperature of the flame is high enough to overcome the barrier to generate the $NH_4^+$ ion. However, the energy barrier in the case of the molecular beam system must be a crucial factor to affect the dissociation reaction of the $[NO(NH_3)_n]^+$ ion. Therefore, on the basis of our observations, it would seem that the dissociation reaction of $[NO(NH_3)_n]^+$ ion follows channel 2.

The ionization potential (IP) of NO[20] is smaller than that of ammonia[26] by 0.895 eV. Therefore, it is anticipated that the positive charge in the mixed cluster ions will be located on the NO moiety. Tomoda and Kimura[27] have reported, on the basis of ab initio calculations, that the electronic ground state of the ammonia dimer cation is a complex of the form $H_3NH^+\cdots NH_2$. That is, an ion−dipole complex is formed between the $NH_4^+$ ion and a $NH_2$ radical. For unprotonated ammonia cluster ions,

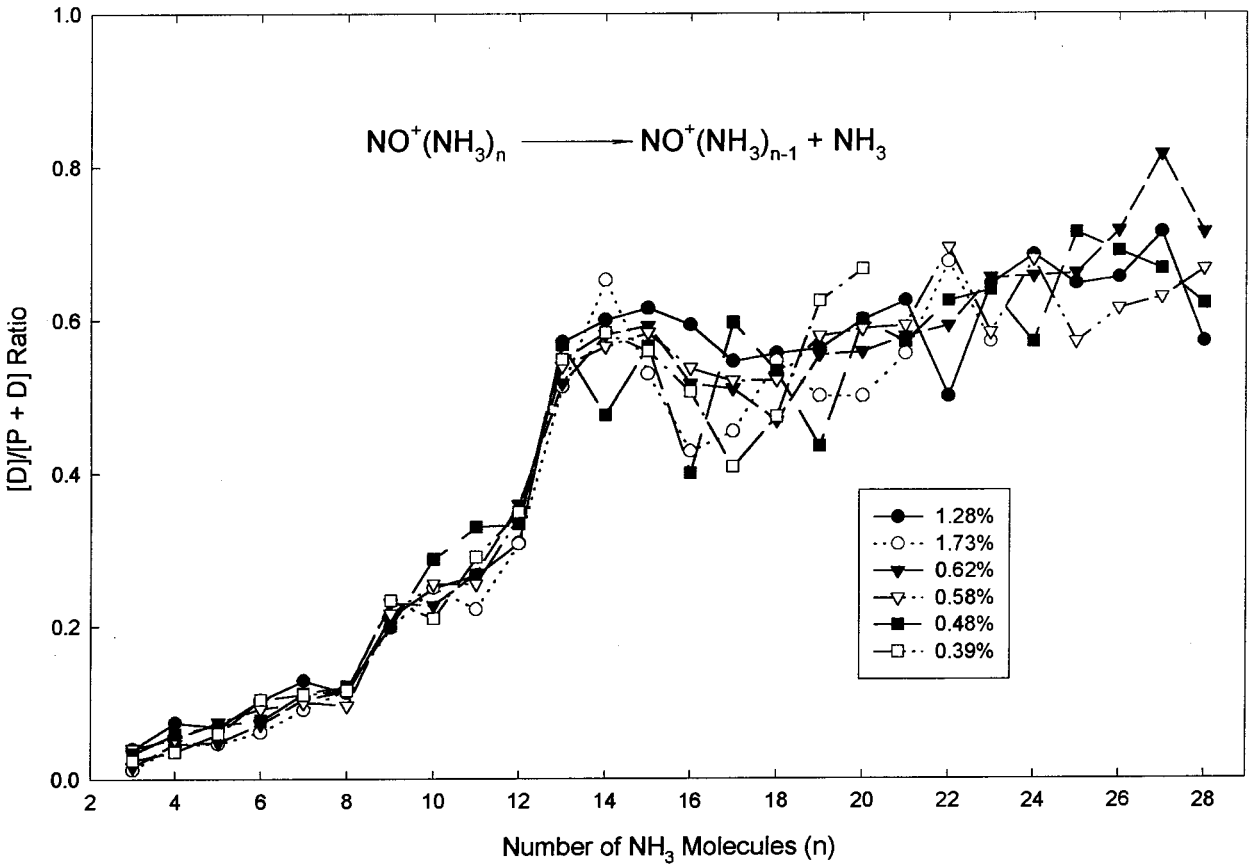


**Figure 3.** Metastable decay ratios [D]/[P + D] for the evaporation of one ammonia molecule from the mixed cluster ion $NO^+(NH_3)_n$ as a function of the ammonia cluster size. Note the abrupt increase in the intensity at $n = 13$.

Shinohara et al.[28] have observed a magic number at $n = 5$, which would suggest a structure such as $(NH_3)_3NH_4^+\cdots NH_2$. In previous MPI experiments,[29] we too have observed unprotonated ammonia cluster ions $(NH_3)^+_{n=1-16}$, where the intensities of the unprotonated cluster ions drop abruptly from $n = 5$ to $n = 6$, again due to the enhanced stability of $(NH_3)_5^+$. From the above results, if the charge of the mixed cluster $[NO(NH_3)_n]^+$ ions was on the ammonia moiety, the magic number of $[NO(NH_3)_n]^+$ should appear at $n = 4$ and have a structure analogous to $(NH_3)_5^+$. However, the magic number is observed to be $[NO(NH_3)_{12}]^+$ instead of $[NO(NH_3)_4]^+$.

Very recently, Aschi and Grandinetti have calculated the stabilization energy for the association reaction, $NH_3 + NO^+ \rightarrow H_3N\cdots NO^+$, whose enthalpy change is evaluated as −30.7 kcal/mol.[19] This value is larger than those of $H_3N^+\cdots NH_3$ (−18.1 kcal/mol)[30] and $NH_4^+\cdots NH_3$ (−24.8 and −21.5 kcal/mol)[31,32] complexes. In addition, the stabilization energy of the $NH_4^+\cdots NO$ (see notes of Table 1) complex will be smaller than that of $NH_4^+\cdots NH_3$, because both the dipole moment (1.47 D)[33] and the polarizability (2.26 Å$^3$)[33] of ammonia are greater than that (0.153 D and 1.70 Å$^3$)[33] of NO. Hence, if the structure of $[NO(NH_3)_n]^+$ resembles that of $(NH_3)_{n+1}^+$, the $(NH_3)_n^+$ cluster as a daughter ion should be observed since the loss of NO from $[NO(NH_3)_n]^+$ is more favorable than that of $NH_3$. However, we observe only the loss of $NH_3$ from $[NO(NH_3)_n]^+$ (as shown in Figure 1). And we feel this result confirms that the positive charge in $[NO(NH_3)_n]^+$ is indeed localized on the NO.

The detailed structure of these mixed cluster ions cannot be determined solely from our present experiments. For the stepwise hydration of the $NO^+$ ion,[34−37] ab initio molecular orbital calculations suggest that, due to the greater magnitude of the positive charge on the nitrogen as opposed to the oxygen (0.548*e* against 0.452*e* for the extended polarized basis set), there is a preference for the water molecules to be bound to the nitrogen rather than to the oxygen atom, up to the third water molecule.[36,37] Choi et al.[37] have proposed, on the basis of spectroscopic evidence for $NO^+(H_2O)_n$, that the smaller clusters for $n \leq 3$ are complexes of $H_2O$ solvent bound to $NO^+$ core ion. For $n \geq 4$, however, the species they observe are of the form $(H_2O)_{n-1}H^+\cdots HONO$ where the central ion, $H_3O^+$, is surrounded by three water molecules as a first solvation shell and the HONO molecule is bound to one of the first solvation shell water molecules. Very recently, Ye and Cheng[38] have reported the calculated structure of $NO^+(H_2O)_n$ for $n \leq 3$ where the most stable isomer for $n = 2$ and 3 is found to have a structure in which the water molecules hydrogen bond to themselves rather than add to the $NO^+$ ion. In comparison to the case of the NO/$H_2O$ cluster, the structure of the $NO^+(NH_3)_n$ cluster ions has the $NO^+$ central ion surrounded by ammonia molecules. If the structure of the $NO^+(NH_3)_n$ cluster ions resembled that of $NO^+(H_2O)_n$ for $n \geq 5$, we would expect to observe a magic number corresponding to the "stable" structure, $(NH_3)_4H^+\cdots H_2NNO$. The $H_2NNO$ moiety is postulated for the NO/$NH_3$ system by comparison to HONO in the NO/$H_2O$ system. Based on theoretical and experimental studies,[1−3,39] the initially generated $H_2NNO$ would also be expected to undergo a dissociation reaction mainly through the two pathways 1 and 2. The binding energy between the $NO^+$ and $NH_3$ (30.7 kcal/mol)[19] is much larger than that between the $NO^+$ and $H_2O$ (19.3 kcal/mol),[40] while the hydrogen bonding energy of ammonia dimer (2.8 kcal/mol)[41] is smaller than that of water dimer (5.4 kcal/mol).[42] Therefore, we think that the structural difference between two systems may be attributed to the differences in the energetics of the interactions. From the above

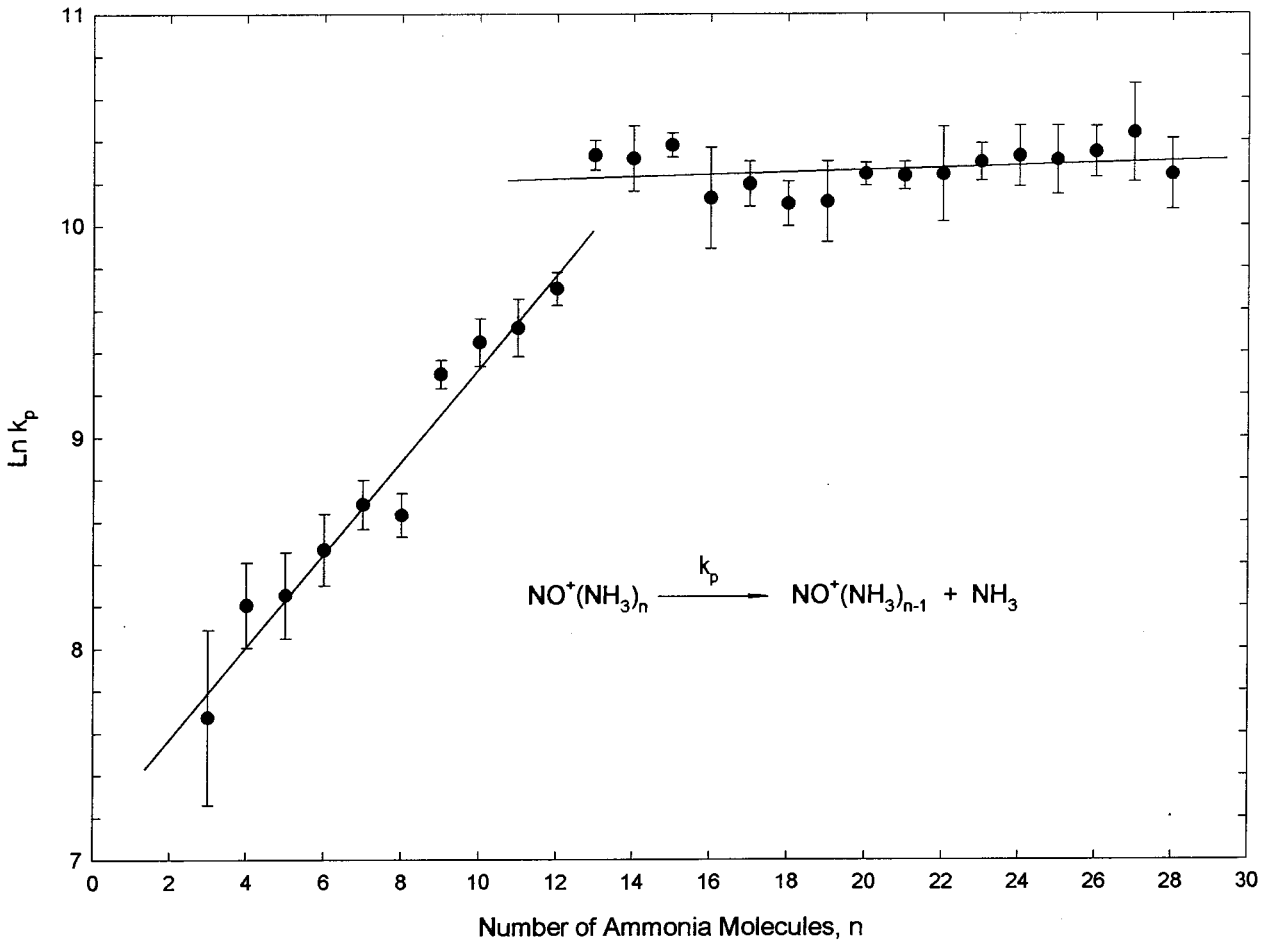


**Figure 4.** Dissociation rate constants for the evaporation of one ammonia molecule from the mixed cluster ions $NO^+(NH_3)_n$ as a function of cluster size. The error bars indicate the standard deviation obtained from the measurements made at six different concentrations of ammonia. The linear curve fitting of rate constants as a function of cluster size is represented by the solid line, showing two different slopes.

**TABLE 1: Relative Energies[a] for Possible Dissociation Channels of the $NO^+(NH_3)_2$ Ion**

| reactions | $\Delta E_{rel}$ (kcal/mol) |
|---|---|
| $NO^+(NH_3)_2 \rightarrow NH_4^{+b} + NH_2NO^c$ (1) | 0.00 |
| $\rightarrow NO^+NH_3^c + NH_3^b$ (2) | 10.4 |
| $\rightarrow NH_4^+NO^d + NH_2^b$ (3) | 44.2 |
| $\rightarrow (NH_3)_2^{+e} + NO^b$ (4) | 45.8 |

[a] The lowest energy channel 1 is set to zero energy for comparison. [b] From ref 59. [c] From ref 19. [d] Calculated on the basis of the reaction $NH_4^+ + NO \rightarrow NH_4^+NO$. For this reaction, the energy change is calculated to be −4.2 kcal/mol at the UHF/6-31G** level of theory. Combining this value with the experimental heats of formation of $NH_4^+$ and NO, the heat of formation of $NH_4^+NO$ is evaluated to be 168.6 kcal/mol. [e] Estimated on the basis of the reaction $NH_3^+ + NH_3 \rightarrow (NH_3)_2^+$. For this reaction, the energy change is found to be −18.1 kcal/mol (ref 30), which gives the heat of formation as 194.1 kcal/mol.

results, we expect that the cluster ions, $[NO(NH_3)_n]^+$, have a central core corresponding to $NO^+$, to which the other ammonia ligands are bound.

In general, the origin of magic numbers in cluster ions can often be attributed to the dynamics of evaporation processes as well as the relative stabilities of the cluster ions and the neutral distribution.[26] There have been a number of experimental[21,43−46] and theoretical[22,47,48] studies on mixed cluster ions of the type $X^+Ar_n$ where X is either an atom or a polyatomic molecule. In the case of a spherical $X^+$ such as Ar, Xe, Al, and I, magic numbers below $n < 20$ have been observed at $n = 12$ and 18. The proposed structure can be interpreted as a central ion surrounded by Ar's to generate an icosahedral structure with a filled solvation shell.

The observation of metastable decay patterns removes any ambiguity that may be present in a traditional mass spectrum ascribed to causes such as differences in the ionization cross section of various ions or the presence of a stable neutral precursor.[24] Therefore, an efficient method of extracting stability information is to observe the daughter ion spectrum. Changes in the ratio of daughter ion to parent ion are a strong indication of the presence of a magic number. As shown in Figure 3, a sudden drop between $n = 7$ and $n = 9$ and a sudden increase between $n = 12$ and $n = 14$ are seen in the intensity distribution of the metastable decay for the mixed cluster ions $NO^+(NH_3)_n$. These features point to the anomalously low ($n = 8 \rightarrow n = 7$) and high ($n = 13 \rightarrow n = 12$) efficiencies for the metastable processes, respectively. Therefore, we deduce the existence of two magic numbers at $n = 8$ and 12 from the metastable decay efficiency on the microsecond time scale.[25,48,49] Here it is very interesting to note that the dissociation channel of $NO^+(NH_3)_6 \rightarrow NO^+(NH_3)_5 + NH_3$ does not show low efficiency although the $NO^+(NH_3)_6$ cluster ion has an anomalously high intensity in the parent mass spectrum. This indicates that the $NO^+(NH_3)_6$ magic number is due to a kinetic stability below the microsecond time scale and not to any thermodynamic stability of the ion itself.[25] The lack of any indication of thermodynamic stability of the $NO^+(NH_3)_6$ ion in the metastable decay analysis, despite the high intensity in the Figure 1 parent spectrum, serves to demonstrate the value of the metastable decay analysis.

The observation of a magic number at $n = 12$ can be explained by closure of the first solvation shell analogous to the inert gas structures even though the central NO ion and surrounding ammonia are not isotropic. Therefore, we propose that there is a successive coordination of ammonia molecules up to $n = 12$ to generate a structure that may resemble a "loose" icosahedron. We believe that there are two main driving forces behind the generation of the first solvation shell: (1) the ion−dipole interaction between the ion core and the solvent molecule and (2) the hydrogen bonding between the solvent molecules. As the cluster size of the first solvation shell increases, the ion−dipole interaction will be decreased, while the hydrogen-bonding interaction will be increased. The 13th ammonia and successive molecules are bound to the ammonia molecules of the first solvation shell. As a result, the ammonia ligands of the first solvation shell bind strongly to the central $NO^+$ ion through two driving forces, while those of the second shell are bound less strongly to the first solvation shell only through hydrogen bonds. This observation is in accordance with the result of an X-ray study of solid ammonia[50,51] in which it is concluded that each ammonia molecule is surrounded by 12 neighbors. In addition, several groups[52−54] have also postulated an icosahedral structure as a complete solvation shell about a dimeric central ion in the benzene cluster system.

In RTOFMS, two experimental values are needed to get information on the binding energy of the cluster ion as a function of the cluster size: (1) the heat capacity and (2) the kinetic energy release (KER).[52−58] The measured metastable decay efficiency is fitted using the heat capacity $C_n$ and the Gspann parameter $\tau$ to get the experimental heat capacity of the cluster ions.[55−58] Klots has proposed that the Gspann parameter $\tau$, defined as $\Delta E_{eva}/kT$, is nearly independent of the composition of the aggregate and cluster size at high cluster sizes.[58] As shown in Figure 4, the rate coefficients beyond $n = 13$ (second solvation shell) are nearly constant, indicating that Klots' postulate is reasonable at larger cluster size. If one considers that the binding energy of the cluster ions is not largely changed at high cluster sizes, the temperature of the cluster surface also may not change as a function of cluster size. However, below $n = 12$ in this study, the rate coefficient is a strong function of the cluster size, indicating that the Gspann parameter $\tau$ may also be strongly dependent on the cluster size.[55,56,58] Previously, Castleman's group[55,56] has performed a calculation to get information on the binding energy by using the modified Gspann parameter as a function of cluster size.

## Conclusion

In this study we have investigated the $NO/NH_3$ mixed cluster ions through multiphoton ionization time-of-flight mass spectrometry. The most prominent mixed cluster ions are found to be $NO^+(NH_3)_n$ and their daughter ions. The analysis of the daughter ions generated from the metastable decay of the mixed cluster ions of the form $NO^+(NH_3)_n$ shows that the predominant dissociation pathway is the loss of one $NH_3$ to generate $NO^+(NH_3)_{n-1} + NH_3$. The rate constant for the metastable decay of $NO^+(NH_3)_n$ to generate $NO^+(NH_3)_{n-1} + NH_3$ increases with increasing cluster size up to $n = 13$ and thereafter nearly is constant, indicating the complete first solvation shell is achieved at $n = 12$.

**Acknowledgment.** We acknowledge the support of the National Science Foundation through Grant NSF/ATM-9711381. D.N.S. is grateful to the Korea Science and Engineering Foundation (KOSEF) for partial financial support and Korea Research Institute of Standards and Science (KRISS). The authors thank reviewers for useful comments.

## References and Notes

(1) Lyon, R. K. *Environ. Sci. Technol.* **1987**, *21*, 231.
(2) Miller, J. A.; Fisk, G. A. *Chem. Eng. News* **1987** (Aug 31), 22.
(3) Miller, J. A.; Bowman, C. T. *Prog. Energy Combust. Sci.* **1989**, *15*, 287.
(4) Tokunaga, O.; Suzuki, N. *Radiat. Phys. Chem*. **1984**, *24*, 145.
(5) Dinelli, G.; Civitano, L.; Rea, M. *IEEE Trans. Ind. Appl.* **1990**, *26*, 535.
(6) Ohkubo, T.; Kanazaw, S.; Nomoto, Y.; Chang, J.-S.; Adachi, T. *IEEE Trans. Ind. Appl*. **1994**, *30*, 856.
(7) Egsgaard, H.; Carlse, L.; Madsen, J. ∅. *Chem. Phys. Lett.* **1994**, *227*, 33.
(8) Kulkarni, S. A.; Pundlik, S. S. *Chem. Phys. Lett.* **1995**, *245*, 143.
(9) Kung, C.-Y.; Kennedy, A.; Dolson, D. A.; Miller, J. A. *Chem. Phys. Lett*. **1988**, *145*, 455.
(10) Lezius, M.; Scheier, P.; M‰rk, T. D. *Chem. Phys. Lett*. **1992**, *196*, 118.
(11) Poth, L.; Shi, Z.; Zhong, Q.; Castleman, Jr., A. W. *J. Phys. Chem. A* **1997**, *101*, 1099.
(12) Desai, S. R.; Feigerle, C. S.; Miller, J. C. *J. Chem. Phys*. **1992**, *97*, 1793.
(13) Takasu, R.; Fuke, K.; Misaizu, F. *Sur. Rev. Lett.* **1996**, *3*, 353.
(14) Purnell, J.; Wei, S.; Buzza, S. A.; Castleman, Jr., A. W. *J. Phys. Chem*. **1993**, *97*, 12530.
(15) Shinohara, H.; Nish, N.; Washida, N. *J. Chem. Phys*. **1985**, *83*, 1939.
(16) Peifer, W. R.; Coolbaugh, M. T.; Garvey, J. F. *J. Chem. Phys.* **1989**, *91*, 6684.
(17) Lykety, M. Y.; Xia, P.; Garvey, J. F. *Chem. Phys. Lett*. **1995**, *238*, 54.
(18) Xia, P.; Hall, M.; Furlani, T. R.; Garvey, J. F. *J. Phys. Chem*. **1996**, *100*, 12235.
(19) Aschi, M.; Grandinetti, F. *Chem. Phys. Lett.* **1997**, *267*, 98.
(20) Linn, S. H.; Ono, Y.; Ng, C. Y. *J. Chem. Phys*. **1981**, *74*, 3342.
(21) Saenz, J. J.; Soler, J. M.; Garcia, N. *Chem. Phys. Lett*. **1985**, *114*, 15.
(22) Harberland, H. *Surf. Sci.* **1985**, *156*, 305.
(23) Boesl, U.; Weinkauf, R.; Schlag, E. W. *Int. J. Mass. Spectrom. Ion Processes* **1992**, *112*, 121.
(24) Stace, A. J.; Moore, C. *Chem. Phys. Lett*. **1983,** *96*, 80.
(25) Lethbridge, P. G.; Stace, A. J. *J. Chem. Phys*. **1988**, *89*, 4062.
(26) Castleman, Jr., A. W.; Tzeng, W. B.; Wei, S.; Morgan, S. *J. Chem. Soc., Faraday Trans*. **1990**, *86*, 2417.
(27) Tomoda, S.; Kimura, *Chem. Phys*. **1983**, *82*, 215.
(28) Shinohara, H.; Nishi, N.; Washida, N. *J. Chem. Phys.* **1985**, *83*, 1939.
(29) Xia, P.; Lyktey, M. Y. M.; Garvey, J. F. *J. Chem. Phys.* **1994**, *101*, 10193.
(30) Ceyer, S. T.; Tiedemann, P. W.; Mahan, B. M. Lee, Y. T. *J. Chem. Phys.* **1979**, *70*, 14.
(31) Meot-Ner, N.; Speller, C. V. *J. Phys. Chem*. **1986**, *90*, 6616.
(32) Keesee, R. G.; Castleman, Jr., A. W. *J. Phys. Chem. Ref. Data* **1986**, *15*, 1011.
(33) Lide, D. R. *CRC Handbook of Chemistry and Physics*, 71st ed.; CRC Press: Boca Raton, FL, 1990−1991.
(34) French, M. A.; Hills, L. P.; Kebarle, P. *Can. J. Chem.* **1973**, *51*, 456.
(35) Stace, A. J.; Winkel, J. F.; Lopez, R. B.; Upbam, J. E. *J. Phys. Chem.* **1994**, *98*, 2012.
(36) Pullman, A.; Ranganathan, S. *Chem. Phys. Lett.* **1984**, *107*, 107.
(37) Choi, J.-H.; Kuwata, K. T.; Hass, B.-M.; Cao, Y.; Johnson, M. S.; Okumura, M. *J. Chem. Phys.* **1994**, *100*, 7153.
(38) Ye, L.; Cheng, H.-P. *J. Chem. Phys.* **1998**, *108*, 2015.
(39) Mebel, A. M.; Lin, M. C. *Int. Rev. Phys. Chem.* **1997**, *16*, 249.
(40) Burdett, N. A.; Hayhurst, A. N. *J. Chem. Soc., Faraday Trans. 1* **1982**, *78*, 2997.
(41) Duguette, D.; Ellis, T. H.; Scoles, G.; Watts, R. O.; Klein, M. L. *J. Chem. Phys.* **1978**, *68*, 2533.
(42) Reimers, J.; Watts, R. O.; Klein, M. L. *Chem. Phys.* **1982,** *64*, 95.
(43) Stace, A. J. *Chem. Phys. Lett.* **1985**, *113*, 355.
(44) Ozaki, Y.; Fukuuyama, T. *Int. J. Mass Spectrom. Ion Processes* **1989**, *88*, 227.
(45) Hobub-Krappe, E.; Gantefor, G.; Broker, G.; Ding, A. *Z. Phys. D* **1988**, *10*, 319.
(46) Whetten, R. L.; Schriver, K. S.; Persson, J. L.; Hahn, M. Y. *J. Chem. Soc., Faraday Trans.* **1990**, *86*, 2375.
(47) Bohmer, H.-U.; Peyerimhoff, S. D. *Z. Phys. D* **1989**, *11*, 239.
(48) Ens, W.; Beavis, R.; Standing, K. *Phys. Rev. Lett.* **1983**, *50*, 27.

(49) Echt, O.; Kreisle, D. K.; Knapp, M.; Recknagel, E. *Chem. Phys. Lett.* **1984**, *108*, 401.
(50) Olovsson, J.; Templeton, D. H. *Acta Crystallogr.* **1959**, *12*, 832.
(51) Loveday, J. S.; Nelmes, R. J.; Marshall, W. G.; Besson, J. M.; Klotz, S.; Hamel, G. *Phys. Rev. Lett.* **1996**, *76*, 74.
(52) Schriver, K. E.; Paguia, A. J.; Hahn, M. Y.; Honea, E. C.; Camarena, A. M.; Whetten, R. L. *J. Phys. Chem.* **1987**, *91*, 3131.
(53) Ernstberger, B.; Krause, H.; Neusser, H. J. *Ber Bunsen-Ges. Phys. Chem.* **1993**, *97*, 884.
(54) Ohashi, K.; Adachi, K.; Nishi, N. *Bull. Chem. Soc. Jpn.* **1996**, *69*, 915.
(55) Wei, S.; Tzeng, W. B.; Castleman, Jr., A. W. *J. Chem. Phys.* **1990**, *93*, 2506.
(56) Shi, Z.; Ford, J. V.; Wei, S.; Castleman, Jr., A. W. *J. Chem. Phys.* **1993**, *99*, 8009.
(57) Lifshitz, C.; Louage, F. *Int. J. Mass Spectrom. Ion Processes* **1990**, *101*, 101.
(58) Klots, C. E. *J. Phys. Chem.* **1988**, *92*, 5864.
(59) Lias, S. G.; Bartmess, J. E.; Liebman, J. F.; Holmes, L.; Levin, R. D.; Mallard, W. G. *J. Phys. Chem. Ref. Data* **1988**, *17* (Suppl. 1).